Smart and Green ACC: Energy and Safety Optimization Strategies for EVs

Sagar Akhegaonkar, Lydie Nouvelière, Sébastien Glaser, and Frédéric Holzmann

***Abstract*—Minimum energy expense and maximum safety with some comfort characterizes the definition of ideal human mobility. Recent technological advances in the autonomous vehicle driving systems not only enhance the safety and/or comfort levels but also present a significant opportunity for automated eco-driving. In this regard, a longitudinal controller for a smart and green autonomous vehicle (SAGA) is investigated. In principle, it is an eco-adaptive cruise control which aims at minimizing energy expenditure and maximizing energy regeneration. This paper presents detailed energy and powertrain analysis through the simulation of specific SAGA application concepts such as, dynamic programming-based offline acceleration optimization for a battery electric vehicle, or SAGA as a supervisory controller in combination with equivalent consumption minimization strategy for a hybrid electric vehicle. The main focus is on the evaluation of a vehicle energy manager which autonomously controls the longitudinal motion while actively balancing efficiency and safety. The comfort is not directly addressed in the conception but regarded as a quality criterion.**

***Index Terms*—Autonomous vehicle control, electric vehicle, energy efficiency, powertrain operation strategy, regenerative braking, vehicle safety**

I. Introduction

INTELLIGENT transportation has become the need of the day. Global warming, unexpected climate changes, dwindling energy resources and unprecedented amounts of air pollution have become some critical problems. They highlight the significance of the efforts toward reducing the carbon footprint of the human mobility to a sustainable level. On the other hand, higher levels of safety and comfort also provide an impetus for the development of the next generation of vehicles. To fulfill such demands, the vehicle of future must be both, smart and green. In this context, substantial research has been done in the recent past on three main fronts, namely, vehicle motion control to enhance safety and/or comfort, propulsion systems to save energy, and navigation-communication systems to improve the vehicle guidance. A state-of-the-art focused on these points is discussed in the following.

Several steps to reach a smart and green vehicle (safe and efficient) have been taken during the last three decades. Traffic studies were undertaken in order to solve the problem of congestion or long monotonous trips that may become source of fatigue and irritation. The Eureka PROMETHEUS project [1] was one of the early demonstrators of the fully automated road vehicle. The French ARCoS project [22] defined several functional levels to improve road safety by adopting a global approach based on a vehicle-infrastructure-driver interaction system. In the continuity, PReVENT, and HAVEit EU integrated projects [23], [24] developed several new advanced driving assistance systems (ADASs) concepts mainly based on vehicle control with a higher level of automation to develop and validate the next ADAS generation. In addition to this, a significant advancement in on board computing capacity has enabled real time image processing such as object/edge detection, recognition, classification, and tracking using vehicle mounted cameras. This presents a possibility to apply automated lateral and longitudinal control for a road vehicle [2], [3]. Furthermore, several projects like CVIS and SAFESPOT were aimed at developing new ADAS by using communication and navigation systems [25], [27] especially by developing the electronic horizon (eHorizon) needed to have a sufficient knowledge of the on-coming road situation.

Research projects like eCoMove [4] and EcoDriver [5] particularly focus on coaching the driver toward an energy efficient driving by modifying the driver behavior.

On the other hand, the trend in vehicle propulsion systems is toward electrification and hybridization. Each modern power train topology presents its own efficiency characteristics and hence it must be carefully evaluated in order to operate as efficiently as possible.

Also, considering the use of communication and navigation systems, a "connected vehicle" equipped with an eHorizon system is an important supplement to the basic energy management system [26]. With the "vehicle to vehicle" (V2V) and "vehicle to infrastructure" (V2I) communication concepts, it is now possible to access to relevant traffic data useful for reducing the energy consumption [8], [9]. Digital maps and eHorizon provide additional remote traffic information.

Manuscript received November 6, 2015; revised January 9, 2016; accepted July 27, 2016. Date of publication September 13, 2016; date of current version December 14, 2017. This work was supported by the European Union FP7-2010-ICT-GC Framework Program in collaboration with INTEDIS GmbH & Company KG, Germany, IFSTTAR/COSYS-LIVIC, France, and the University of Evry-Val-d'Essonne, France, under Grant 258133. This paper was recommended by Associate Editor L. L. Lai.

S. Akhegaonkar is with the University of Evry-Val-d'Essonne, F91020 Évry, France (e-mail: sagar.akhegaonkar@ens.univ-evry.fr).

L. Nouvelière is with the University of Evry-Val-d'Essonne, IBISC Laboratory, F91020 Évry, France (e-mail: lydie.nouveliere@ibisc.univ-evry.fr).

S. Glaser is with IFSTTAR/COSYS-LIVIC Institute, F78000 Versailles, France (e-mail: sebastien.glaser@ifsttar.fr).

F. Holzmann is with INTEDIS GmbH, 97084 Würzburg, Germany (e-mail: frederic.holzmann@intedis.com).

Color versions of one or more of the figures in this paper are available online at http://ieeexplore.ieee.org.

Digital Object Identifier 10.1109/TSMC.2016.2600273

Primitive systems like curve warning systems, intelligent speed adaptation, and cooperative adaptive cruise control are already in implementation phases [10].

The following sections aim at presenting a new ADAS named smart and green autonomous vehicle (SAGA) for smart and green adaptive cruise control (ACC). It is developed on the base of these three fields, namely, safety enhancement, energy saving, and V2V or V2I communication. SAGA concentrates on autonomously generating the longitudinal control commands with the objective to balance safety and efficiency applied to a light vehicle. In this context, the scope of operation for SAGA not only covers the efficient acceleration and regeneration in a battery electric vehicle (BEV) [6] but also the supervisory control over the core power train controller in a hybrid electric vehicle (HEV) [7]. Since SAGA is a longitudinal motion controller, it must adapt its generic concept to take into account the different characteristics of the specific power train topology. The SAGA system then attempts to use such information to determine efficient acceleration and deceleration maneuvers taking into consideration near and remote traffic conditions, thereby maximizing the energy regeneration subject to the power train component limitations.

Rather than an application specific controller, SAGA must be seen as a broader concept which can be adapted to the specific power train configurations. This paper attempts to demonstrate how such a concept can be adapted to a BEV, HEV, and plug-in HEV (PHEV). The benefits over the conventional mobility systems are shown through several dedicated scenarios simulations for energy and safety analysis. This paper is organized as follows. Section II presents an overview of the vehicle and energy models with their components and configuration details; it is followed with a concept definition of the SAGA system. In Section IV, the development of SAGA on a BEV is discussed while Section V is fated to present its application on HEV and PHEV and is followed by a conclusion.

II. Vehicle Models for Energy Analysis

Vehicle models for conventional battery electric and HEVs are developed in Simulink. They are used to simulate and compare the energy consumption of different power trains in conjunction with the SAGA function. All three models are based on a prototype of the "TATA Indica" vehicle used in the eFuture project [11]. The specifications of the prototype are listed in Table I. A detailed description of the models is given in the following sections.

A. Battery Electric Vehicle

A description of the Simulink-based model for the BEV can be found in [12]. It is a twin-motor front axle driven vehicle powered by a lithium-ion battery. A 15-kW permanent-magnet synchronous motor e-Motor module with a 750-Nm peak torque is modeled. The motor model is based on look-up tables which define the speed-torque characteristics and also the power losses corresponding to the operating point of the motor. The look-up tables are generated through the actual

TABLE I
Vehicle Specifications

M_v	Vehicle Mass BEV/ HEV-PHEV/ Conventional	 *1550/1550/1350 kg*
A	Front area	*2.28 m^2*
C_w	Drag co-efficient	*0.36*
f_r	Co-efficient of rolling resistance	*0.015*
r	Wheel radius	*0.3 m*
Motor Max. Torque Max. Speed		PMSM axial flux, high speed with reduction gear *750 Nm* *1200 rpm*
Battery HEV/ PHEV/ BEV		Li-ion, NMC chemistry *7/13/26 kWh*

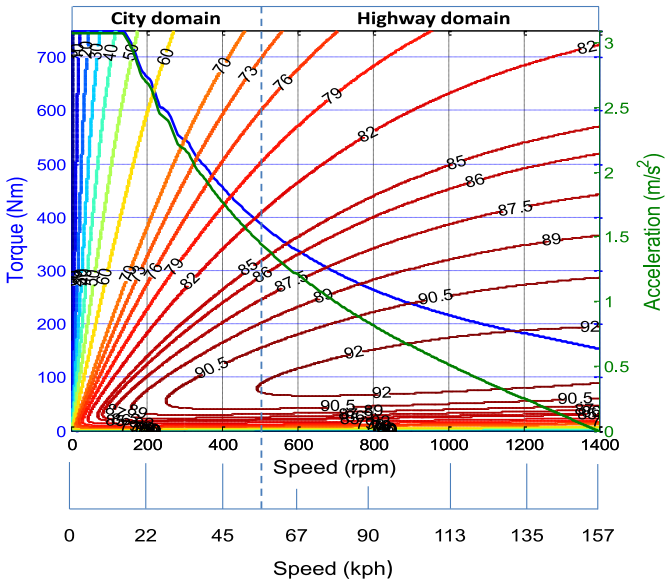

Fig. 1. Motor torque-speed-efficiency characteristics.

measurement of the motor performance over its operating range (0−1200 rpm).

The torque-speed characteristics for the e-Motor is shown in Fig. 1 along with the efficiency map and the maximum possible acceleration (using 2 such motors) on a flat road for the prototype vehicle. Hence, a total maximum torque of 1500 Nm is available. The maximum acceleration is calculated taking into consideration the vehicle data in Table I.

The motor map can be divided into two operation domains depending on the speed, namely, city and highway. The motor has an integrated reduction gear. It can be observed that the gearing adjusts the torque-speed characteristics to obtain a maximum possible efficiency.

The energy storage system (ESS) is a lithium-ion (NMC chemistry) battery developed as a part of the eFuture project by Miljøbil Greenland AS. The model is based on a virtual circuit as defined in [13] which represents the battery

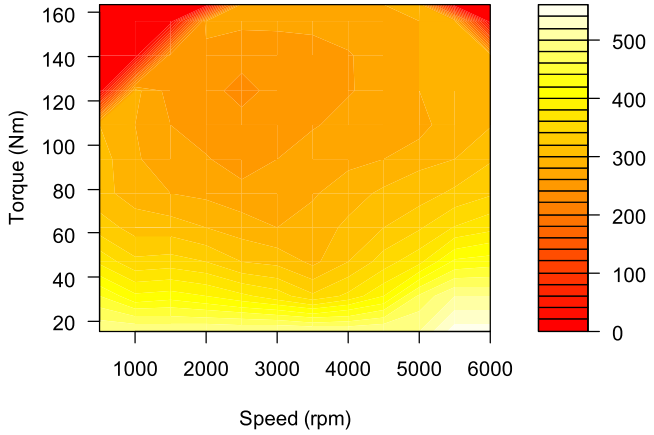

Fig. 2. IC engine efficiency map in g/kWh.

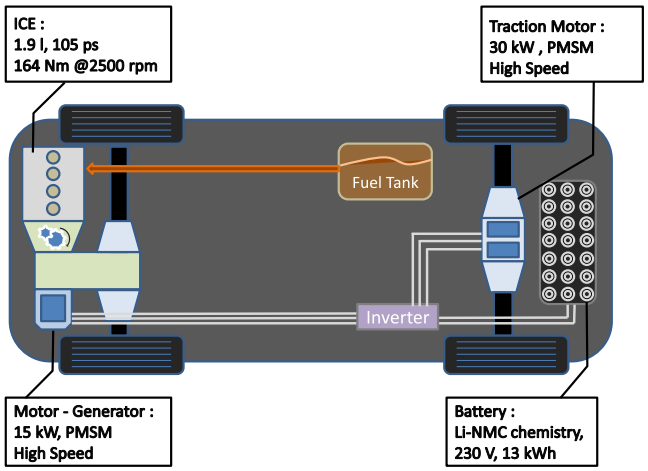

Fig. 3. Schematic representation of a TtR hybrid.

capacity, internal resistance, and transient behavior of the battery. A temperature dependent internal resistance variation is taken into consideration while calculating the power loss and efficiency. Inverter losses are assumed negligible.

B. Conventional Vehicle

A model for a conventional vehicle is realized by modifying the BEV model, replacing its power train system and redefining the vehicle mass. Thereby a 1.9-liter, 105-ps gasoline engine is modeled based on its fuel consumption behavior. The base efficiency engine map containing the static "specific fuel consumption" in g/kWh is shown in Fig. 2. It is used to determine the final energy consumption in liters/100 km.

A 5-speed manual transmission is modeled which complements the internal combustion (IC) engine torque-speed characteristics. Since the gear selection is controlled by an intelligent energy management algorithm [7], it may as well be classified as a semi-automatic transmission. The gear ratios in increasing respect are 3.250, 1.950, 1.423, 1.033, and 0.730. The final gear ratio is 4.063 and it yields the total drive ratio for each gear as a product with individual gear ratios.

C. Hybrid Electric Vehicle

The HEV model is realized by combining the BEV and conventional vehicle power trains and adding a power-split definition block. In this paper, a through the road (TtR) power-split hybrid model is used for analysis. The TtR hybrid allows more flexible power-split operation as compared to a normal planetary geared system owing to the fact that the front and rear powered axles are mechanically isolated except TtR. Hence, the control algorithm may freely choose the operating points for engine and motor depending on the best efficiency region. A schematic representation of the TtR hybrid is shown in Fig. 3.

Such a TtR hybrid is defined with the following equations:

$$u_{\text{split}} = T_{\text{eM}}/T_{\text{total}} \tag{1}$$

$$T_{\text{total}} = F_x \cdot r \tag{2}$$

$$T_{\text{eM}} = u_{\text{split}} \cdot T_{\text{total}} \tag{3}$$

$$T_{\text{ice}} = \left(1 - u_{\text{split}}\right) T_{\text{total}}/g_{\text{ice}} \tag{4}$$

where u_{split} is the power-split ratio, T_{total} is the required torque, T_{eM} is the torque demanded from the electric motor, T_{ice} is the torque demanded from the IC engine, g_{ice} is the total drive ratio, and F_x is the resistance force at the wheel with r as wheel radius.

D. Generic Energy Model

For the energy calculation, backward looking vehicle models are developed, i.e., the vehicle velocity profile is assumed as known and based on that, the energy consumption is calculated. Specific to the power train system, the energy supply may be from combustion engine or battery or the combination of both. Following that (5)–(7) define the energy calculations:

$$F_x = \left(\frac{C_w.\rho \cdot A \cdot v^2}{2} + M_v \cdot g \cdot f_r + M_v \cdot g \cdot \sin\beta + M_v \cdot a\right) \tag{5}$$

$$P_x = F_x \cdot v \tag{6}$$

$$E_x = \int P_x dt \tag{7}$$

where M_v is the vehicle mass, A is the front area, C_w is the drag co-efficient, f_r is the co-efficient of rolling resistance, r is the wheel radius, a is the vehicle acceleration, v is the vehicle velocity, ρ is the air density, β is the grade angle, F_x is the required force at the wheel, P_x is the required power, and E_x is the required energy, the required energy E_x must be supplied by the power sources and hence the efficiencies of the power train system must be taken into consideration. Therefore for a sample time dt, where $E_{\text{batt.dis/chg}}$ is the battery discharge or charge energy, η_{eM} is the motor efficiency, $\eta_{\text{batt.dis/chg}}$ is the battery discharge or charge efficiency, P_{eM} is the motor power, E_{ice} is the energy from IC engine, and η_{ice} is the IC engine efficiency

$$E_{\text{batt.dis}} = P_{\text{eM}} dt/(\eta_{\text{eM}} \cdot \eta_{\text{batt.dis}}) \tag{8}$$

$$E_{\text{batt.chg}} = P_{\text{eM}} \cdot \eta_{\text{eM}} \cdot \eta_{\text{batt.chg}} dt \tag{9}$$

$$E_{\text{ice}} = P_{\text{ice}} dt/\eta_{\text{ice}}. \tag{10}$$

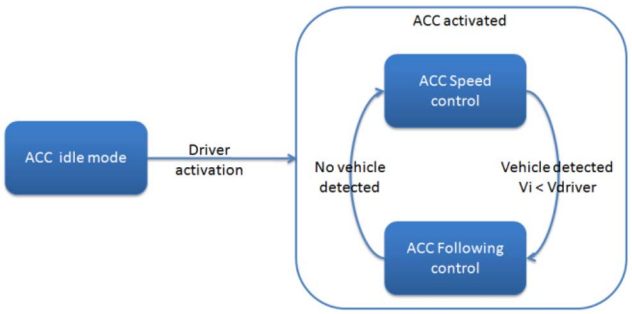

Fig. 4. SAGA: modes of operation.

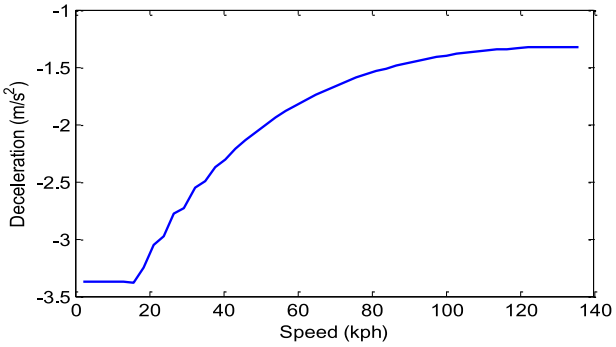

Fig. 5. Deceleration capacity of the motor.

III. SAGA Concept and Problem Definition

The SAGA concept, originally coined as the smart and green ACC, is described in detail in [14]. It is further extended to a full speed range ACC (FSRA) for a BEV in [6] and for an HEV in [7]. The idea is to reprogram a normal cruise control to take into account efficiency and safety. The possibility to combine this concept with the electric propulsion, regeneration systems, and automated vehicle motion control enables a true eco-driving performance. There are two basic modes of the SAGA function as shown in Fig. 4. When there is no obstructing vehicle in the motion path then it must follow the driver desired speed with respect to the legal speed limits; this is the "speed control mode." In case of an obstructing vehicle being present, the SAGA must follow the front vehicle at a safe headway spacing in the "distance control mode." SAGA must also respect the ISO ACC performance requirements [15] such as the average automatic deceleration of ACC systems shall not exceed 3.5 m/s^2 (except emergency), while the acceleration is limited to 2 m/s^2, the average rate of change of an automatic deceleration (jerk) shall not exceed 2.5 m/s^3. In this context, SAGA must only be activated above 7 m/s.

A. Speed Control Mode

This mode is active in the phase where there is no front detected vehicle. As there is no interaction with other road users in this mode, it is not mainly safety critical. In this mode, SAGA behaves like a classical ACC. In some cases, the acceleration is directly proportional to the velocity difference between actual and function desired speeds. In others, the acceleration may be optimized. Similarly, the deceleration is optimized for maximizing the recuperation. For both, acceleration and deceleration, SAGA must follow the standard performance guidelines as defined in [15].

B. Distance Control Mode

This mode is activated upon the detection of a front vehicle. Normally, the sensor range is 150 m. This headway spacing can be further divided in two subphases: the "speed equalization phase" where the ego vehicle approaches the front vehicle and decelerates in order to equalize speeds; after this, the ego vehicle follows the front vehicle with a constant headway spacing. In the distance control mode, the objective is to regulate the error on the headway clearance e_d ($e_d = d - T_d V$) around 0, where d is the clearance to the lead vehicle, T_d is the desired time headway, and V is the ego vehicle speed. The algorithm can be made more robust by including the relative speed ΔV into the control equation. The resulting acceleration is the control output defined by these two errors

$$a = K_{\text{cv}} \cdot \Delta V + K_{cd} \cdot (d - T_d V). \tag{11}$$

In order to recuperate maximum energy from the deceleration maneuver, it is proposed that the exclusive motor braking be used. However, at higher speeds, the motor braking capacity decreases as seen in Fig. 5, where the deceleration capacity for the eFuture prototype is calculated taking into consideration the air drag and wheel resistance.

Hence, it may not be possible to ensure the same level of safety as in conventional ACC strategy which applies normal service brakes. The main reasons for this are: first, for instance during the initial deceleration maneuver where the ego vehicle approaches the front vehicle which is moving with a lower velocity or decelerating then, if the required deceleration for velocity equalization is more than the maximum motor braking capacity, then surely, any collision cannot be avoided. Second, during the constant velocity or the headway spacing sustaining phase (distance control mode), if the front vehicle undergoes a very strong deceleration then it may not be possible to equalize the speeds only with the help of the motor braking. Therefore, some changes in the conventional ACC algorithm are suggested in [28]. For an extreme use case where the initial time headway is 2 s, the ego vehicle speed is 130 kph, and the front vehicle speed is 60 kph, the possible options are as follows.

1) Exclusive Motor Braking: Owing to a limited motor brake capacity, it is needed to increase the minimal safe time headway. However, to obtain the same safety, it is also needed to increase the minimal time headway up to 5 s. The resulting distance is hardly achievable as the sensor range is limited and other road users may cut in the space between vehicles.

2) Threshold Braking Strategy: To switch to a conventional braking if the time headway drops below a given threshold. For instance, we can maintain a collision free system, as for a conventional ACC, with an initial time headway of 3.7 s and an activation of a stronger braking at a threshold on the time headway of 1.5 s.

3) Optimized Blended Braking: Use blended braking (motor and conventional) over the operating range. It evaluates a safety factor at each instant and controls this value

below a threshold using excess conventional brakes over the motor brakes. This will allow a better traffic fluidizing with a headway spacing of 2 s without compromising the safety.

While the small headway spacing may pose safety risks, a large headway spacing allows for vehicle cut-in, whereas using conventional brake results in a wastage of energy which could be regenerated. This forms the basic problem definition for the SAGA function. The above approaches are further investigated in [6], [14], and [28]. In this paper, we summarize these investigations and describe the comprehensive scope of applications and feasibility of the SAGA function in the following sections.

IV. SAGA as Applied to BEV

In [6], the application of SAGA as an FSRA in both city and highway scenarios is discussed. As seen in Fig. 1, the BEV power train operation map can be divided into city and highway domains. These domains distinctly exhibit different characteristics not only with respect to the efficiency and torque capacity but also the acceleration-deceleration frequencies and constant speed characteristics of collective surrounding traffic. Hence, two different strategies have been developed, each for the respective scenarios.

A. Dynamic Programming-Based Acceleration Controller for the City Domain

A city traffic domain is characterized with frequent acceleration and braking events and has a comparatively low average velocity. The BEV power train uses two modules of the motor model. Its capability to achieve high acceleration values owing to its high torque capacity in the city domain is obvious in Fig. 1. It is also evident that the high acceleration area is not the best efficiency region. The acceleration energy is stored into the vehicle as a momentum which is dissipated through road resistance, air drag, gradient energy requirements, and braking. Then, in a city driving scenario which is characterized by frequent standstill to velocity limit transitions and vice-versa, high accelerations lead to a high average velocity which means some more air drag. Also, a vehicle which undergoes high acceleration stores a large quantum of its battery energy into the vehicle as a momentum. If in such a situation the vehicle must brake then the stored momentum will be wasted as heat or regeneration component losses. According to this philosophy, a very low acceleration value will lead to maximum energy savings. However, it will also lead to a long time duration to cover the same distance. Hence, taking into consideration the power train efficiency behavior in the city traffic, there must be a certain optimum velocity trajectory defined by specific acceleration values which optimizes the energy and time requirements. Thereby, a dynamic programming-based acceleration controller is developed in [6] and [12]. Such a controller is elaborated in the following.

The acceleration phase is discretized in $N+1$ steps of equal $0-N$ distance. If J is the objective function which depends on energy and time, then J can be defined as

$$J = Q1 * \text{Energy} + Q2 * \text{Time} \tag{12}$$

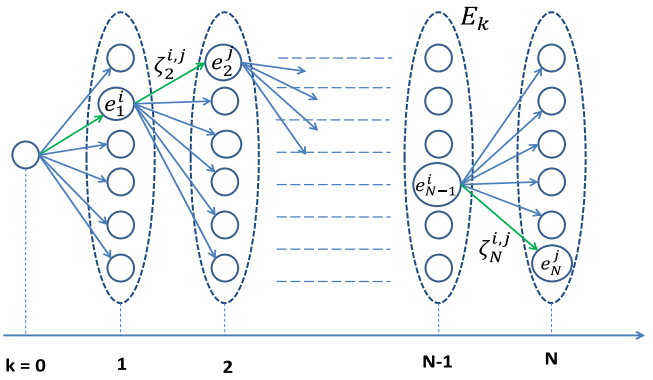

Fig. 6. Formulation of a DP algorithm.

where $Q1$ and $Q2$ are the weight coefficients. Since J is a function of the acceleration which is a function of the motor torque "t" of the vehicle, where $t \in T$, the control problem can be formulated as follows:

$$\min \sum_{k=0}^{N-1} J_{k+1}(T_k),\ T_k \in \left[T_{\text{low}}, T_{\text{high}}\right]. \tag{13}$$

In Fig. 6, e_k^i is the state i at the step k. E_k is the set of the states e_k^i at the step k and is defined by the discretized state space T_k which is a set of motor torque values from $0.1 * T_{\max}Nm$ to $T_{\max}Nm$ with an interval of $0.1 * T_{\max}Nm$. $\zeta_{k+1}^{i,j}$ is the cost associated to each transition from the state $i \in E_k$ to the state $j \in E_{k+1}$. Thus, it can be stated that for a transition from step $k = 1$ to $k = 2$, where the initial state e_1^i at step 1 is already defined, the goal is to find a state $e_2^j \in E_2$ at step 2 where the cost of transition $\zeta_2^{i,j}$ is minimum. This minimum cost is nothing but $J_2(T_1)$ as defined in (12). Therefore, the dynamic programming technique can be defined as follows.

Let $\pi^* = t_0^*, t_1^*, \ldots, t_{N-1}^*$ be an optimal control strategy for this problem, where t is the motor torque value. Suppose that, when the torque t_{k-1}^* is applied, the state e_k^i is reached at time i during the acceleration phase. Considering the subproblem for which, from the state e_k^i at time i, we seek to minimize the cost to go from k *to* N: $J = \Sigma_k^{N-1}\zeta_{k+1}(T_k)$, then the optimal control strategy $\pi^* = t_0^*, t_1^*, \ldots, t_{N-1}^*$ is optimal for that subproblem.

For the transition from every optimum state to the next probable state with a constant applied torque t, the initial and final velocities are recorded along with the time. Thus, the acceleration for the state transition is calculated. Results for optimum values of acceleration depending on cost function J of energy and time for equal distance steps are shown in Fig. 7. The time cost per optimization using dynamic programming (DP)/A-ECMS algorithms (see Section V), in a real time objective, can be largely reduced by considering no longer a time-dependent model but a position-dependent model to apply these algorithms. This is even more necessary when the case of the vehicle inserted in a traffic environment with a safety distance problem is considered, the eHorizon is thus also used. The cost function is normalized to return a value in range of 0−1. Each box represents an optimization process. It can be observed that for a specific sample distance, an optimum

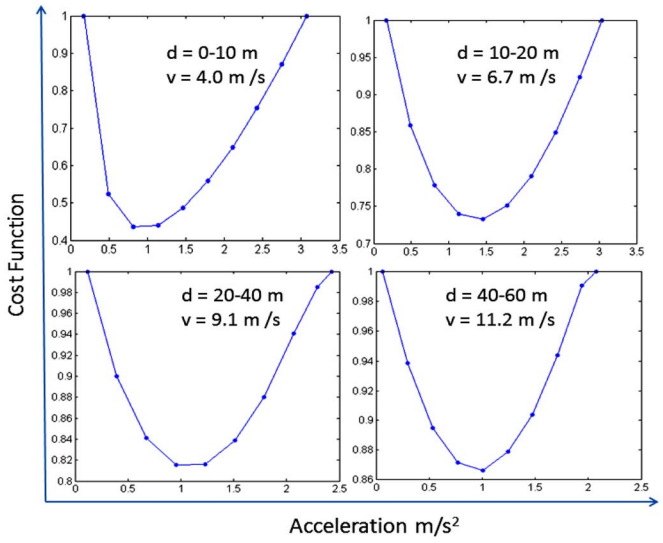

Fig. 7. Cost function results ($Q1 = 1, Q2 = 1$).

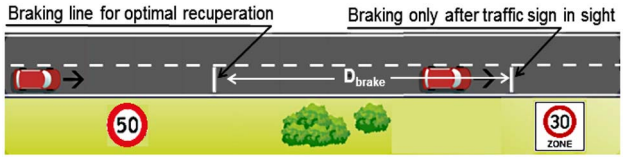

Fig. 8. Braking maneuver (approaching a speed limit).

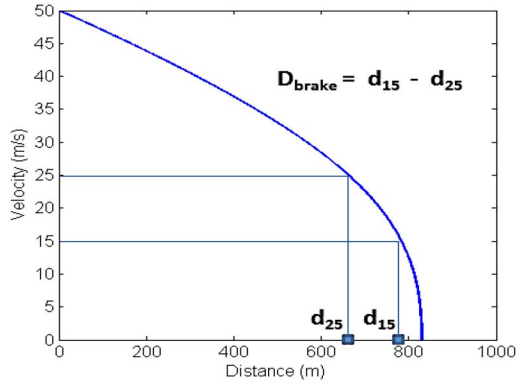

Fig. 9. Optimum braking distance.

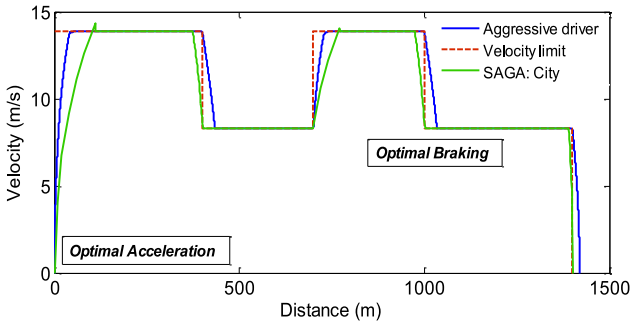

Fig. 10. Optimum velocity profile (city domain).

acceleration value is obtained. The velocity "v" in the boxes is the velocity reached by the vehicle when it covered the given sample distance with the constant optimum acceleration. As the velocity increases the sample distance is also increased so as to optimize approximately 2 s of the drive ahead. It can also be considered that as the velocity increases, the maximum acceleration which corresponds to the control points decreases. Hence, a valid spread of the control parameters for calculating the cost function is achieved.

B. Deceleration Strategy: City Domain

As emphasized before, the city domain traffic consists of frequent acceleration and braking maneuvers. Such events may rise due to different reasons like stop and go traffic, traffic signals, sudden velocity limit changes, intersections, etc. Conventional braking converts the vehicle momentum into some waste friction heat. In a BEV, it is possible to regenerate this deceleration energy by routing it through a motor-generator back into the electrical ESS. However, such a regeneration system is bottlenecked through the component limitation like battery charge acceptance characteristics. Hence, most original equipment manufacturers only employ a small part of total regeneration capacity and waste a significant amount of energy. Recent technology upgrades in the Li-polymer batteries allow better charge acceptance characteristics and could make a full capacity regenerative braking possible. Nonetheless, as already established, an exclusive motor braking has a deceleration capacity limitation. Hence, in a city scenario, to ensure a safe exclusive motor braking, the distance from which braking should be started must be calculated in advance. This concept is explained in Fig. 9.

For a vehicle travelling at 50 kph and approaching a speed limit of 30 kph, a normal driver will brake only after he observed the traffic sign (Fig. 8). However, here, he must use the service brakes which provide a strong braking force.

In order to recover all the energy from this braking maneuver, the motor brake must be used. Since motor brakes are not as strong as service brakes, the braking must begin at a distance D_{brake}. To calculate this distance at a given velocity, the vehicle model was simulated to brake from a velocity of 50 to 0 m/s, exclusively under the influence of motor brakes. The distance D_{brake} can be calculated from these data as shown in Fig. 9. Hence, for example, if a vehicle must brake from 25−15m/s, it must start braking at a distance of $d_{15}-d_{25}$. For this purpose, the location where such braking maneuvers are applicable, e.g., speed limit, traffic signal, traffic jams, etc., must be known in advance. Such information would be available through digital maps, V2V, and V2I communications.

C. City Domain Controller: Simulation and Results

The city domain controller as a part of the SAGA function for BEV is realized by combining the acceleration and deceleration strategies described above. The behavior of such a controller is compared to that of an aggressive driver model as shown in Fig. 10. A nonstandard velocity cycle is defined to reflect the city traffic situation. The controller algorithm is set to follow the dynamic programming-based acceleration till the speed limit be reached. The velocity is maintained at the

speed limit or at the front vehicle one. It can be observed that the velocity profile for DP-based algorithm has a gradual increase in velocity compared to a strong acceleration profile of the driver model. The optimum velocity profile balances the energy consumption and time to travel. Also, since the DP algorithm strategy already knows about the speed limits beforehand, it can start the optimum exclusive braking maneuver earlier. Thereby, it absorbs all the available braking energy which would normally become wasted. It can be observed that the use of maximum motor capacity for braking has resulted into a comparable braking performance to the driver model which is designed to brake with a −750-Nm torque. The total cycle distance is 1400 m which is covered by the driver model in 140 s and the DP algorithm in 145 s. As compared to an earlier algorithm [12], the modified algorithm [6] requires much less time to cover the same cycle because of the increased braking capacity. It is assumed that the driver model can recuperate with −260 Nm (out of total −750 Nm) while DP algorithm uses the full motor capacity for braking. While the driver model requires 0.259 kWh, the DP-based controller requires 0.241 kWh for the same distance, saving approximately 9%-energy. This figure will change depending on the frequencies of acceleration and braking events over the cycle.

D. SAGA Function for BEV Highway Domain

As compared to a city domain, the highway domain distinguishes itself with the high average velocity and less frequent and low acceleration or deceleration maneuvers. As it is evident from Fig. 1, the high speed region of the power train is characterized with superior efficiency and lower acceleration capacity. In this domain, the main energy saving potential lies not in the optimization of acceleration but in the conservation of momentum lost during the deceleration through a maximum regeneration. In this context, given the high velocity, the SAGA speed and distance control strategy described in Section III is applied in highway domain. Thereby, we discuss the optimized blended braking control strategy described in [28]. To balance safety and efficiency, it is necessary to know the system state at each instant. With the given system variables which define the system state, namely, velocity difference ΔV, remaining distance d, and motor capacity, it must become clear at any given instant whether it is possible to safely complete the given deceleration maneuver without compromising the safety. If such a possibility confirmation is not present then the system must be forcibly manipulated into the safe region. This action of steering the system into the safe region is achieved by blending the motor brakes with additional conventional braking.

To determine the system safety status, a safety indicator SI is calculated and the system is tuned to a threshold value of this indicator. If this threshold value is breached then the blended braking is activated. If not, a pure motor braking maneuver is allowed to proceed. With the activation of blended braking, the additional braking is computed from the safety indicator and a proportional control is executed using a gain of $K_b = 10$

$$\mathrm{SI} = \frac{\Delta V}{d} \tag{14}$$

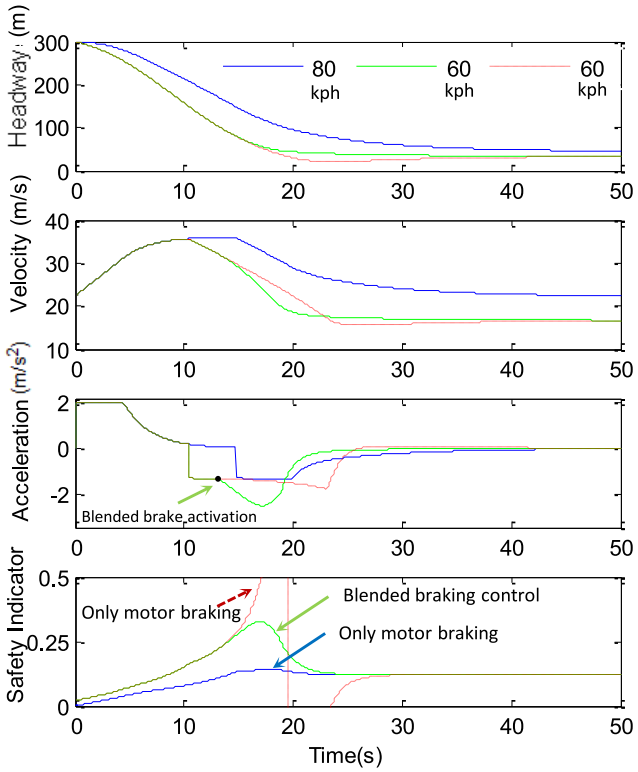

Fig. 11. SAGA deceleration 130−80/60 kph, blended braking control with safety indicator activation at 0.22.

$$a_{\mathrm{blended}} = a_{\mathrm{motor}} + a_{\mathrm{correction}} \tag{15}$$

$$a_{\mathrm{correction}} = -K_b \cdot \mathrm{SI}. \tag{16}$$

In order to ensure enough time for the motor brake to absorb the regeneration energy, it is necessary to activate the motor brake as soon as the front obstacle is detected. Hence, in blended brake SAGA strategy, the gains K_{cv} as 0.75, K_{cd} as 0.1 are accordingly tuned. Fig. 11 demonstrates the performance of the optimised blended braking system. The deceleration phase for 130−80 kph is managed by the motor as expected. Here, the SI does not breach the 0.22 mark and the blended braking is not activated. In case of a deceleration phase for 130−60 kph, the activation barrier is breached. If no action is taken then SI quickly rises (in red) to indicate any safety risk. It is seen that without any intervention, although the maneuver is completed without any collision, the headway spacing has dropped dangerously close. At front vehicle speeds lower than 40 kph, a collision is inevitable. At the activation limit breach, the blended braking is activated (in green), an additional braking power is applied with conventional brakes, and SI is suppressed to the safe position. The introduction of this safety indicator also implies a comfortable driving situation during a braking maneuver.

Among Fig. 12, a jerk plot with SAGA activated is illustrated with a low average and the presence of a few high peaks. The ACC standard guidelines allow a jerk to be under 2.5 m/s^3 (in absolute value) in average and the presence of peaks with an amplitude above this limit provided they last less than 1 s so as to remain in an acceptable comfort area (less than 0.15 s for Fig. 12). The conception of SAGA does not directly balance

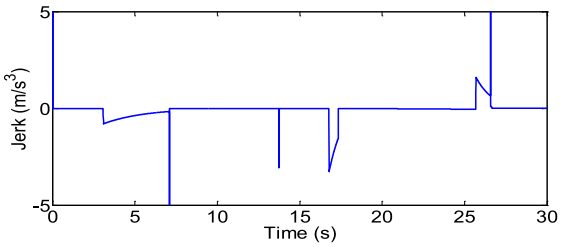

Fig. 12. Jerk illustration for an SAGA scenario.

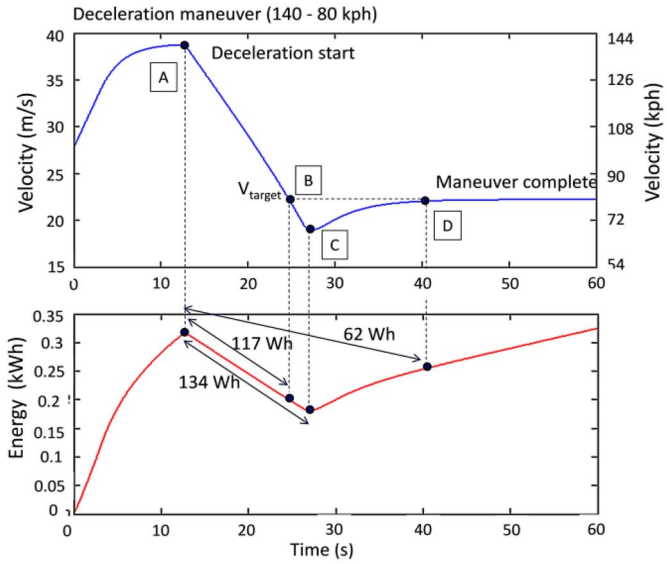

Fig. 13. SAGA test result analysis for a deceleration maneuver.

the comfort with the safety and efficiency criteria but this one is naturally induced by the ACC-based system.

A Pareto 80/20 analysis shows that 80% of braking which contains a high potential of recoverable energy is during the slow front vehicle approach, highway construction, speed limits, and traffic signals. The evaluation of the benefits of using SAGA in these situations is done making an energy analysis as shown in Fig. 13. Here, a deceleration maneuver from 140 to 80 kph (slow front vehicle approach) is analyzed using ego vehicle velocity and recovered energy data. During deceleration, the ego vehicle already achieves the target velocity of 80 kph at point B. However, as the distance from front vehicle is less than 2 s, the vehicle undergoes further deceleration till point C and readjusts till point D to achieve the 2 s headway. This results in multiple values for recovered energy analysis. While this phenomenon is also present in 130−80 kph maneuver with less intensity, it completely disappears in 140−100 kph maneuver, where points C and D are absent. For a fair comparison, the energy between points A and B is considered. Thereby, for 140−80 kph maneuver about 219 Wh of kinetic energy (KE) is depleted from which, 50.5 Wh is spent to overcome air drag and 23.3 Wh is spent to overcome wheel resistance. Out of the remaining 145.2 Wh, the regenerative braking system absorbs 117 Wh at an efficiency of 80.5%. Table II gives an idea of the recoverable KE for some other maneuvers.

TABLE II
ENERGY RECOVERY POTENTIAL FOR VARIOUS MANEUVERS

Braking Maneuver	Recovered Energy (Wh)	K.E depletion (Wh)	Time (sec)
140 – 80 kph	117	219	27
130 – 80 kph	95	174	22
140 – 100 kph	68.5	159	20
100 – 60 kph	57.5	106	20
50 – 0 kph	24	41	6

Fig. 14. eFuture prototype for SAGA function test.

E. GACC Testing

In the context of the European Union funded project "eFuture," a preliminary version of SAGA function was tested at the Gaydon test track in U.K. For this purpose, the eFuture BEV prototype (Fig. 14) with real time measurement equipment, front cameras, radar sensors, and a data fusion box is used.

A part of test sequence is discussed in the following. The main aim of testing was to demonstrate system ability to sense front vehicle and control ego vehicle with respect to the SAGA function. It must be noted that the eFuture vehicle prototype has a software regulated inherent regenerative torque limitation due to battery charge acceptance limits. This limits the regeneration torque to about −260 Nm and hence, at this stage of development, the actual strategy of SAGA function to employ strong exclusive motor brakes cannot be evaluated in this testing. Nonetheless, the control part consisting of sensing and actuation is successfully evaluated and validated.

As seen in Fig. 15, at about 34 s, the data fusion box is activated and the system acknowledges the front vehicle presence. The SAGA function senses the small headway of about 25 m and the front vehicle deceleration. It requests a deceleration of about -2 m/s^2. It is seen that the vehicle has answered with a deceleration of about -1 m/s^2. At about 55 s when the headway is sufficiently increased, SAGA tries to equalize the speeds. From 70–80 s the controller chattering is evident while it tries to regulate the speed. As the front vehicle increases its speed, SAGA tries to follow. However, some power train

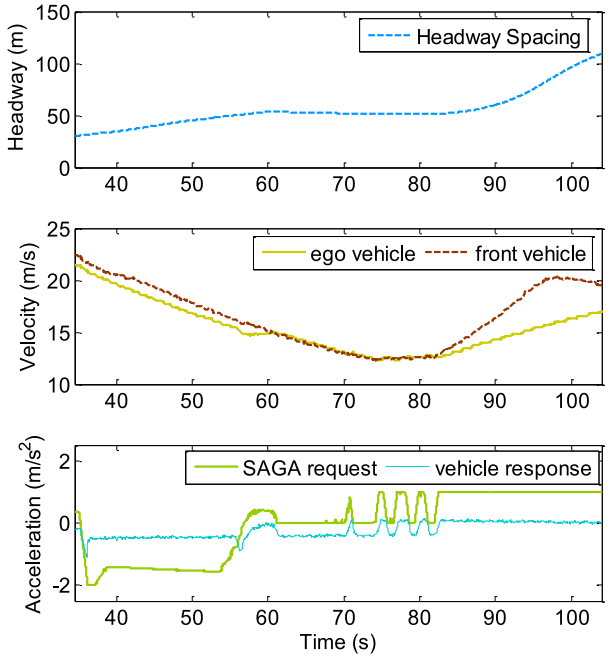

Fig. 15. SAGA test result analysis.

controller software problems need to be sorted out since the requested torque is not being supplied.

V. SAGA as Applied to HEV and PHEV

Unlike the BEV, a direct control of the power train through SAGA is not possible in the HEV or PHEV. In a BEV, the SAGA determines the acceleration or deceleration values which can be directly translated into the torque demand for the power train. This is possible because a single power supply source is being controlled. In HEV or PHEV, even if the SAGA can determine the acceleration and deceleration values, i.e., the torque demanded from the power train, this one being itself comprised of two power sources, hence, it is also necessary to control the power-split for the respective power demand. Thereby, a bi-layered control system is proposed where SAGA acts a supervisory controller over a core power train controller. For a power-split hybrid topology as described in Fig. 3, the equivalent consumption minimization strategy (ECMS) [16] is investigated as a core power train controller in [7]. The details of this investigation are elaborated in the following sections. In order to understand the operation of an SAGA-ECMS bi-layered control, it is necessary to briefly understand the ECMS concept.

A. Equivalent Consumption Minimization Strategy

The concept of ECMS was developed in [16]. It is based on optimal control theory and can be derived from Pontryagin's minimum principle. In this paper, ECMS is used as a direct power train control algorithm in combination with the SAGA function for efficient autonomous vehicle control. The aim is to minimize the fuel consumption and sustain the battery charge level. It is explained as follows:

$$E_{\text{total}} = E_{\text{ice}} + E_{\text{batt}} \tag{17}$$

where, E is for energy. But all the energy ultimately comes from the fuel, even the electrical energy E_{batt} which is stored in battery is produced by the motor-generator powered by IC engine running at a specific operating point. If this operating point is known then there can be a direct comparison between fuel energy and electrical energy. This comparison factor is $s(t)$ and is called "equivalence factor." For the rate of energy consumption it can be stated that

$$\dot{m}_{\text{fuel}} = \dot{m}_{\text{ice}} + s(t) \cdot \dot{m}_{\text{batt}} \tag{18}$$

$$\dot{m}_{\text{fuel}} = \dot{m}_{\text{ice}} + s(t) \cdot \frac{E_{\text{batt}}}{Q_{\text{lhv}}} \cdot \dot{\text{soc}}(t) \tag{19}$$

$$\dot{m}_{\text{fuel}} = \dot{m}_{\text{ice}} + s(t) \cdot \frac{P_{\text{eM}}}{Q_{\text{lhv}}} \tag{20}$$

where $\dot{\text{soc}}(t)$ is the change in battery state of charge, m is the fuel mass and Q_{lhv} is the lower heating value of gasoline in MJ/g. The aim is to minimize the cost function J, i.e., the total fuel cost m_{fuel} subject to operational constraints as

$$\begin{aligned} \text{Min} \quad & J(u_{\text{split}}, g_{\text{ice}}) = \int_0^T \dot{m}_{\text{fuel}}(t)dt \\ \text{subject to} \quad & P_{\text{total}} = P_{\text{ice}} + P_{\text{eM}} \\ & P_{\text{ice.min}} \le P_{\text{ice}}(t) \le P_{\text{ice.max}} \\ & P_{\text{eM.min}} \le P_{\text{eM}}(t) \le P_{\text{eM.max}} \\ & P_{\text{gen.min}} \le P_{\text{gen}}(t) \le P_{\text{gen. max}} \\ & \text{SOC}_{\text{min}} \le \text{SOC}_{\text{batt}}(t) \le \text{SOC}_{\text{max}}. \end{aligned} \tag{21}$$

In order to minimize the fuel consumption in the driving mission of time T, the global optimization problem is reduced to an instantaneous minimization problem by discretizing it into smaller time segments. For each segment the optimum values for u_{split} and g_{ice} must be determined such that the optimum fuel consumption is obtained without violating the SOC constraints.

As stated earlier, the equivalence factor allows a direct comparison between fuel and electrical energy for known engine operating point and overall system efficiency. Thus, if $s(t)$ is high then the ECMS tries to penalize the use of electrical energy. On the other hand, if $s(t)$ is low the use of electrical energy is encouraged. Since at any instant, the future operating point of the system is unknown, it is not possible to find the conversion between the electrical energy being spent which will be replenished by fuel energy at a later time or electrical energy being generated which will compensate the fuel energy later. But if a driving cycle is known *a priori* then it is possible to find a lumped efficiency parameter for an electrical and fuel energy conversion which is a characteristic of that particular velocity cycle. Such a method is described in [17] where two values of $s(t)$ are derived applicable to charging (s_{chg}) or discharging (s_{dis}) battery efficiencies. In [18], it is shown that only one equivalence factor suffices in ECMS. This $s(t)$ is always located between s_{chg} and s_{dis} values. However, this $s(t)$ only offers an optimum performance for the respective velocity cycle. Any deviation in the velocity cycle will result in a suboptimal and noncharge sustaining behavior.

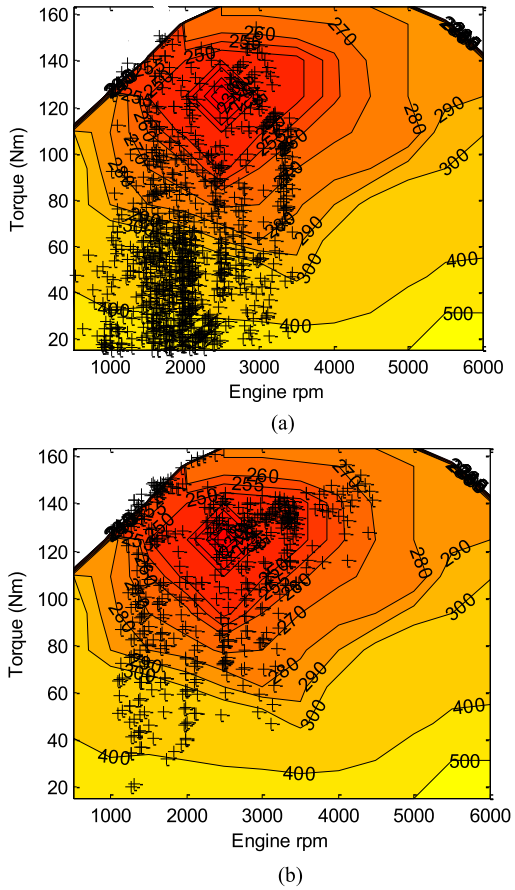

Fig. 16. (a) WLTP class3 cycle engine operating points. (b) Conventional ice (left), TtR ECMS.

Hence, a normal ECMS cannot be applied in real time. In [18], an adaptive ECMS (A-ECMS) concept was introduced. Since then, many different methods were introduced which used a real time update for the equivalence factor. Such an algorithm facilitates a constant adaptation of the strategy based on battery SOC status. One such method is described in [19] and applied as follows:

$$s(t) = s_0 + s_0 \cdot K \cdot \tan\left(\frac{\text{soc}_{\text{ref}} - \text{soc}(t)}{2\pi}\right) \tag{22}$$

where s_0 is the nominal equivalence factor. Since we know that equivalence factors lie between s_{chg} and s_{dis}, the nominal equivalence factor may be derived as an average of the two. K is a feedback factor, it decides for which $s(t)$ correction intensity related to the soc deviation from soc_{ref}. K is manually tuned to obtain an acceptable performance of the system.

The A-ECMS is implemented and tested for both charge sustaining normal HEV and blended mode PHEV. While for normal HEV the soc_{ref} does not change, in a PHEV the aim is to use as much battery as possible. Hence, the soc_{ref} must be adjusted according to the covered distance. For a PHEV

$$\text{soc}_{\text{ref}(t)} = \left(\frac{\text{soc}_{\text{final}} - \text{soc}_{\text{init}}}{D_{\text{total}}}\right) \cdot d(t) + \text{soc}_{\text{init}} \tag{23}$$

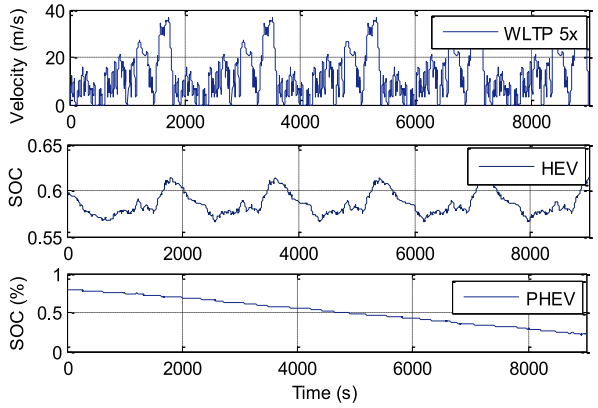

Fig. 17. ECMS controller behavior for HEV and PHEV on a WLTP cycle.

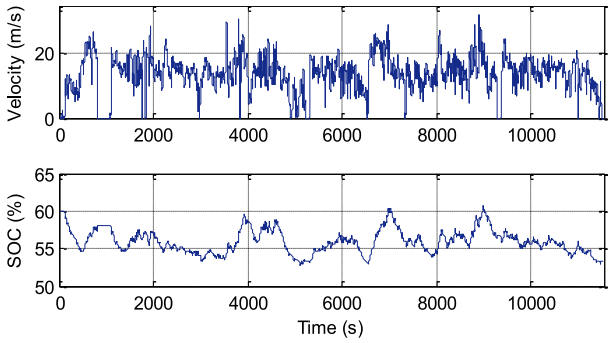

Fig. 18. ECMS controller behavior on a real world recorded velocity session.

B. ECMS Controller Behavior

The A-ECMS algorithm is developed as a MATLAB *s*-function and implemented in the Simulink model of the TtR hybrid. Simulation are made in order to compare power train performance of conventional, HEV and PHEV topologies on the worldwide harmonized light vehicles test procedures (WLTPs) class 3 cycle [20] and further tested with a completely different set of random velocity points which are recorded during a real world driving [21]. The value of s_0 is finally manually tuned to 3.5. The value of K was manually tuned to 0.7. soc_{ref} is fixed at 60%.

As observed in Fig. 16, in which the engine operating points for conventional and TtR hybrid over a single WLTP cycle are compared, ECMS optimizes the fuel consumption by shifting the points in low efficiency region to high efficiency region. In Fig. 17, the behavior of ECMS controller is shown as applied to WLTP class 3 cycle which is repeated 5 times for a total distance of 116 km. It can be seen that ECMS successfully sustains SOC within certain limits for a charge sustaining pure HEV. Whereas, for a plug-in hybrid, the full utilization of battery energy between SOC levels 0.8–0.2 is ensured.

For this it is necessary that the trip distance must be known beforehand. Apart from SOC regulation the aim of ECMS is to reduce the consumption. ECMS actively avoids the engine operation points of lower efficiency as seen in Fig. 16, where a single run of WLTP cycle is compared for ECMS hybrid and conventional ICE.

In Fig. 18, ECMS is applied on an actual recorded velocity session (Arco_Merano) [21] spanning about 157 km.

TABLE III
FUEL CONSUMPTION FOR VARIOUS POWER TRAIN CONFIGURATIONS

Velocity Cycle	Power train	Consumption (l/100km)
WLTP class3 (5x)	Conventional ICE	6.68
WLTP class3 (5x)	Pure HEV (CS)	5.52
WLTP class3 (5x)	Plug-in HEV (Blended)	3.23
Real world (A_M)	Conventional ICE	5.54
Real world (A_M)	Pure HEV (CS)	4.19
Real world (A_M)	Plug-in HEV (Blended)	1.96

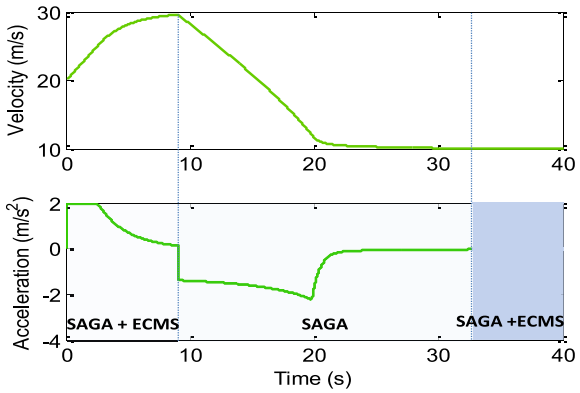

Fig. 19. Bi-layered SAGA and ECMS controller operation.

ECMS regulates the SOC within a certain range and reduces the fuel consumption.

Table III gives an overview of different consumptions figures for respective power trains and cycles. A charge sustaining hybrid saves about 17% in WLTP cycle and about 24% in the Arco_Merano velocity session compared to the conventional ICE vehicle which is given an advantage of 200 kg weight reduction and an efficient gear shifting algorithm which maintains the demand on most efficient engine map patch. It is not fair to compare the performance of plug-in hybrids since they use externally refillable electric energy.

C. SAGA as Supervisory Controller for HEV and PHEV

As previously established, the longitudinal control for an HEV or PHEV must be a bi-layered system wherein SAGA function and ECMS controller behave in a kind of master–slave system. The SAGA function defines the longitudinal motion characteristics. These are passed on to the ECMS controller which further defines the power train operation properties. Such a bi-layered control for hybrid power train is elaborated in the following.

Fig. 19 demonstrates a maneuver where the desired set speed is 30 m/s and actual speed is 20 m/s. The front vehicle is 300 m ahead and sensor range is 150 m, so the SAGA function determines an acceleration value in speed control mode. The approximate amount of torque to achieve the specified acceleration is calculated and passed on to the ECMS function. Depending on the system parameters, ECMS determines the power-split, transmission gear and amount of torque to be generated or consumed (stored as electrical energy) for each power train component. In short, for the acceleration domain SAGA acts as a superficial command generator whereas ECMS manages the actual power train activity.

At a headway spacing of 150 m, SAGA senses the front vehicle and shifts into distance control mode. The front vehicle is moving at 10 m/s. SAGA determines if the motor braking capacity is sufficient to achieve the required deceleration within a safe headway distance. Otherwise the service brakes are engaged as seen in case of classical ACC. ECMS is held dormant during this time and SAGA directly controls the regenerative power components. When the speed of ego vehicle is equalized with the front vehicle, the objective is to follow the front vehicle speed. In this operation domain characterized with constant speed and intermittent acceleration, SAGA again performs the supervisory control with ECMS as the active power train controller.

VI. CONCLUSION

Through this paper, a generic concept for an autonomous vehicle longitudinal motion control is proposed. The final function and its adaption to various power train configurations have been evolved from the basic smart and green ACC which is expanded methodically. It is observed that the SAGA function has varied impact on energy saving which is subject to the power train configuration and velocity cycle. For a BEV in the city environment, SAGA can save about 9% whereas the each deceleration maneuver in the highway environment can save about 30–130 Wh subject to situation probabilities. Similarly, for an HEV, an ECMS strategy in combination with SAGA function saves about 17% as compared to a conventional vehicle running on a WLTP cycle. However, these figures only reflect certain specific scenarios-based savings and will change depending on various factors. Here, it is significant that each maneuver successfully managed by SAGA ensures a specific quantity of saved energy and an accumulation of such events leads to a substantial amount of energy saving.

REFERENCES

[1] *EUREKA Project E45 PROMETHEUS*. Accessed on Mar. 25, 2014. [Online]. Available: http://www.eurekanetwork.org/project/-/id/45

[2] J. Levinson *et al.*, "Towards fully autonomous driving: Systems and algorithms," *in Proc. IEEE Intell. Veh. Symp. (IV)*, Baden-Baden, Germany, 2011, pp. 163–168.

[3] M. Bertozzi *et al.*, "Equipment and capabilities of the vehicles for the VisLab intercontinental autonomous challenge," in *Proc. GIRPR*, Trento, Italy, 2012.

[4] *eCoMove Project*. Accessed on Mar. 25, 2014. [Online]. Available: http://www.ecomove-project.eu

[5] *ecoDriver Project*. Accessed on Mar. 25, 2014. [Online]. Available: http://www.ecodriver-project.eu

[6] S. Akhegaonkar, S. Glaser, L. Nouveliere, and F. Holzmann, "Smart and green ACC series: A city and highway specific approach towards a safe and efficient eDAS," in *Proc. Elect. Veh. Symp. (EVS-27)*, Barcelona, Spain, Nov. 2013, pp. 1–9.

[7] S. Akhegaonkar, S. Glaser, L. Nouveliere, and F. Holzmann, "Smart and green ACC: As applied to a through the road hybrid electric vehicle," in *Advanced Microsystems for Automotive Applications*. Berlin, Germany: Springer, Jun. 2014, pp. 15–27.

[8] P. Fernandes and U. Nunes, "Vehicle communications: A short survey," in *Proc. IADIS Telecommun. Netw. Syst. Conf.*, Lisbon, Portugal, 2007.

[9] J. D. Vreeswijk, M. K. M. Mahmod, and B. Van Arem, "Energy efficient traffic management and control—The eCoMove approach and expected benefits," in *Proc. 13th Int. IEEE Conf. Intell. Transp. Syst. (ITSC)*, Funchal, Portugal, 2010, pp. 955–961.

[10] IHS SupplierBusiness. (2011). *Advanced Driver Assistance Systems Report IHS Inc.* [Online]. Available: http://www.supplierbusiness.com

[11] *eFuture Project*. Accessed on Mar. 25, 2014. [Online]. Available: http://www.efuture-eu.org/

[12] S. Akhegaonkar *et al.*, "Modeling and simulation of battery electric vehicle to develop an energy optimization algorithm," in *Proc. 11th Int. Symp. Adv. Veh. Control (AVEC)*, Seoul, South Korea, Sep. 2012.

[13] M. Knauff, J. McLaughlin, C. Dafis, and C. Nwankpa, "Simulink model of a lithium-ion battery for the hybrid power system testbed," in *Proc. ASNE Intell. Ships Symp.*, May 2007.

[14] S. Glaser *et al.*, "Smart and green ACC, safety and efficiency for a longitudinal driving assistance," in *Advanced Microsystems for Automotive Applications International Forum AMAA 2013*. Berlin, Germany: Springer, Jun. 2013, pp. 123–133.

[15] ISO 15622:2010. *Intelligent Transport System, Adaptive Cruise Control System, Performance Requirements and Test Procedures*. Accessed on Sep. 2016. [Online]. Available: http://www.iso.org/iso/iso_catalogue/catalogue_tc/catalogue_detail.htm?csnumber=50024

[16] G. Paganelli, S. Delprat, T.-M. Guerra, J. Rimaux, and J. J. Santin, "Equivalent consumption minimization strategy for parallel hybrid powertrains," in *Proc. IEEE 55th Veh. Technol. Conf. VTC Spring*, vol. 4. Birmingham, AL, USA, 2002, pp. 2076–2081.

[17] A. Sciarretta, M. Back, and L. Guzzella, "Optimal control of parallel hybrid electric vehicles," *IEEE Trans. Control Syst. Technol.*, vol. 12, no. 3, pp. 352–363, May 2004.

[18] C. Musardo, G. Rizzoni, and B. Staccia, "A-ECMS: An adaptive algorithm for hybrid electric vehicle energy management," in *Proc. 44th IEEE Conf. Decis. Control (CDC) Eur. Control Conf. (ECC)*, Seville, Spain, Dec. 2005, pp. 1816–1823.

[19] H. Friden and H. Sahlin, "Energy management strategies for plug-in hybrid electric vehicles," M.Sc. thesis, Dept. Signals Syst., Chalmers Univ., Gothenburg, Sweden, 2012.

[20] *Worldwide Harmonized Light Vehicles Test Procedure (WLTP)*. Accessed on Mar. 25, 2014. [Online]. Available: https://www2.unece.org/wiki/pages/viewpage.action?pageId=2523179

[21] *Arco_Merano.mat*. Accessed on Jan. 21, 2014. [Online]. Available: http://www.ecosm12.org/node/21

[22] *ARCoS Project*. Accessed on May 29, 2014. [Online]. Available: http://innovations-transports.fr/Building-databases-for-driving

[23] *PReVENT Project*. Accessed on May 29, 2014. [Online]. Available: http://www.ertico.com/prevent

[24] *HAVEit Project*. Accessed on May 29, 2014. [Online]. Available: http://www.haveit-eu.org

[25] *CVIS Project*. Accessed on May 29, 2014. [Online]. Available: http://www.cvisproject.org/

[26] S. S. Williamson, *Energy Management Strategies for Electric and Plug-in Hybrid Electric Vehicles*. New York, NY, USA: Springer, 2013, pp. 1–253.

[27] *SAFESPOT Project*. Accessed on May 29, 2014. [Online]. Available: http://www.safespot-eu.org/

[28] S. Akhegaonkar, L. Nouveliere, S. Glaser, and F. Holzmann, "Smart and green autonomous vehicle controller: Enhancement of regeneration and powertrain strategy," in *Proc. 12th Int. Symp. Adv. Veh. Control (AVEC)*, Tokyo, Japan, Sep. 2014.

Sagar Akhegaonkar was born in Nagpur, India, in 1984. He received the B.S. degree in mechanical engineering from Pune University, Pune, India, in 2006, the M.Sc. degree in automotive engineering from RWTH Aachen University, Aachen, Germany, in 2011, and the Dr.Phil. degree from the University of Évry Val-d'Essonne, Évry, France, in 2015, in cooperation with Intedis GmbH & Company KG, Würzburg, Germany.

He is currently with AKKA Group, Sindelfingen, Germany.

Lydie Nouvelière was born in Le Mans, France, in 1975. She received the M.Sc. degree in robotics and autonomous systems from the University of Paris VI, Paris, France, in 1999, and the Dr.Phil. degree in robotics and control engineering from the University of Versailles, Versailles, France, in 2002.

She has been an Associate Professor with the University of Évry Val-d'Essonne and IBISC Lab, Évry, France since 2003. From 2007 to 2013, she was a Scientific Adviser with IFSTTAR Institute, Versailles.

Sébastien Glaser received the Dipl.-Ing. degree from the Ecole Nationale des Travaux Publics de l'Etat, Lyon, France, the M.Sc. degree in computer vision from the Université de Saint Étienne, Saint-Étienne, France, in 2001, and the Dr.Phil. degree in automatic control from the Université of Évry Val d'Essonne, Évry, France, in 2004.

He has been with IFSTTAR, Versailles, France since 2001. He is currently a Senior Researcher with Vedecom Institute, Paris, France.

Frédéric Holzmann received the M.Sc. degree from the École Nationale Supérieure de Mécanique et des Microtechnique, Besançon, France, in 2003, and the Dr.Phil. degree in robotics from the École Polytechnique Fédérale de Lausanne, Lausanne, Switzerland, in 2006.

He has been a Chief Technology Officer with Intedis GmbH & Company KG, Würzburg, Germany since 2008.